OPEN ACCESS
JOURNAL OF ADVANCED DIELECTRICS
Vol. 12, No. 6 (2022) 2241002 (10 pages)

DOI: 10.1142/S2010135X22410028

XI'AN JIAOTONG UNIVERSITY
World Scientific
www.worldscientific.com

Domain structure and dielectric diffusion–relaxation characteristics of ternary $Pb(In_{1/2}Nb_{1/2})O_3$–$Pb(Mg_{1/3}Nb_{2/3})O_3$–$PbTiO_3$ ceramics

Xudong Qi[*,¶,**], Kai Li[†], Lang Bian[‡], Enwei Sun[‡], Limei Zheng[§] and Rui Zhang[‡,||,**]

[*]*School of Physics and Electronic Engineering, Harbin Normal University*
Harbin 150025, P. R. China

[†]*Guangdong Provincial Key Laboratory of Electronic Functional Materials and Devices*
Huizhou University, Huizhou 516001, P. R. China

[‡]*School of Instrumentation Science and Engineering, Harbin Institute of Technology*
Harbin 150080, P. R. China

[§]*School of Physics, State Key Laboratory of Crystal Materials*
Shandong University, Jinan 250100, P. R. China

[¶]qixudong0316@126.com
[||]ruizhang_ccmst@hit.edu.cn

Received 8 June 2022; Revised 9 July 2022; Accepted 14 July 2022; Published 18 August 2022

Relaxor-based ternary $Pb(In_{1/2}Nb_{1/2})O_3$–$Pb(Mg_{1/3}Nb_{2/3})O_3$–$PbTiO_3$ (PIN–PMN–PT) single crystals and ceramics are promising candidates for high-performance electromechanical conversion devices. It is known that the domain structure and dielectric diffusion–relaxation characteristics are crucial to the excellent performances of relaxor ferroelectrics. In this work, we prepared the PIN–PMN–PT ceramics with various PIN/PMN proportions and systematically investigated their domain structure and dielectric diffusion–relaxation properties. The effect of PIN/PMN proportion on the domain size and dielectric diffusion–relaxation characteristics was also studied. The investigations showed that PIN–PMN–PT ceramics presented multi-type domain patterns comprising irregular island domains and regular lamellar domains. Moreover, the dependent relations of PIN/PMN proportions on the dielectric diffusion and domain size indicated that the PIN composition has a stronger lattice distortion than PMN composition; increasing the PIN proportion can enhance the dielectric diffusion and decrease the domain size. Our results could deepen the understanding of structure–property relationships of multicomponent relaxor ferroelectrics and guide the design and exploration of new high-performance ferroelectric materials.

Keywords: Piezoelectric ceramics; PIN–PMN–PT; dielectric diffusion and relaxation characteristics; domain structure.

1. Introduction

Relaxor-based ferroelectrics, such as $Pb(Mg_{1/3}Nb_{2/3})O_3$–$PbTiO_3$(PMN–PT) and $Pb(Zn_{1/3}Nb_{2/3})O_3$–$PbTiO_3$ (PZN–PT) single crystals and ceramics, have recently received widespread attention due to their excellent dielectric and electromechanical properties.[1–3] A large piezoelectric coefficient (d) and a high electromechanical coupling coefficient (k) make the relaxor ferroelectrics promising candidates for piezoelectric actuators and sensors, ultrasonic transducers, motors, and undersea applications.[1,4] However, the low Curie temperature (T_C ~ 130–170°C) and rhombohedral (R) to tetragonal (T) phase transition temperature ($T_{\mathrm{R-T}}$ ~ 60–95°C) of PMN–PT crystals severely limit their applications.[5,6] In this case, the performance degradation is inevitable due to the heat generation under a long-time and high-power operating ambient. Introducing the $Pb(In_{1/2}Nb_{1/2})O_3$ (PIN) content is an effective method to enhance the $T_{\mathrm{R-T}}$ and T_C, i.e., broader the temperature usage for PMN–PT systems. The ternary $Pb(In_{1/2}Nb_{1/2})O_3$–$Pb(Mg_{1/3}Nb_{2/3})O_3$–$PbTiO_3$ (PIN–PMN–PT) was reported to possess higher phase transition temperatures compared with those of PMN–PT and PZN–PT systems, while exhibiting a comparable dielectric and electromechanical properties.[5–9]

Hosono *et al*. reported that the morphotropic phase boundary (MPB) of the PIN–PMN–PT systems is a linear composition region between the PIN–37PT and PMN–32PT.[10] Wang *et al*. further studied the phase diagram of PIN–PMN–PT ceramics.[5] Lin *et al*. systematically investigated the dielectric, piezoelectric and electromechanical properties of PIN–PMN–PT ceramics.[6] It was found that the $T_{\mathrm{R-T}}$ is above 100°C, and the T_C varies from 170°C to 320°C for PIN–PMN–PT ceramics.[5–7] Simultaneously, the MPB samples display an excellent dielectric and electromechanical properties of $\varepsilon_r > 3000$, $d_{33} > 500$ pC/N, and $k_p > 60\%$.[5–10] The broad applied temperature range combined with excellent electric properties

**Corresponding authors.

allows the PIN–PMN–PT ceramics to become a promising candidate in high-temperature applications.

Moreover, the PIN–PMN–PT ceramics present a strong diffuse phase transition (DPT) featured by a diffuse permittivity peak and frequency-dependent maximum permittivity (ε_m) around T_m (ferroelectric–paraelectric phase transition temperature).[7–10] Our previous works indicated that a large electrostrictive coefficient and high energy-storage efficiency could be achieved in the ergodic relaxor (ER) phase of PIN–PMN–PT ceramics, which is associated with their strong diffusion–relaxation behaviors.[11] In this case, the diffusion–relaxation behavior encapsulates the dielectric phenomenon of dielectric diffusion featured by a broad dielectric peak and dielectric relaxation characterized by frequency-dependent ε_m around T_m. It is generally known that the dielectric diffusion–relaxation characteristics are crucial to the excellent performances of relaxor ferroelectrics, such as large dielectric permittivity,[12] giant piezoelectricity and large electrostrictive coefficient.[11,13,14] Meanwhile, the dielectric diffusion–relaxation characteristics are closely related to the nucleation and growth of polar nanoregions (PNRs) in relaxor ferroelectrics.[15–17] Thus, the research of diffusion–relaxation characteristics combined with the PNRs' growth kinetics will deepen the understanding of structure–property relationships in PIN–PMN–PT systems.

It is widely recognized that the nanoscale domain structure plays an important role in the dielectric and electromechanical properties of relaxor ferroelectrics.[3,14,18] Unlike the normal ferroelectrics, relaxor ferroelectrics are a type of ferroelectrics where the long-range ferroelectric order is disrupted by intrinsic chemical inhomogeneity and charge disorder, presenting complex polar states at the nanoscale.[19] The unique polar state and the nanosized domain structure contribute to the excellent dielectric, electro-optic and electromechanical properties of relaxor ferroelectrics.[19–21] Albeit many studies focused on the phase structure and electromechanical properties of PIN–PMN–PT crystals, the research on their domain structure and diffusion–relaxation characteristics was lacking. In practical terms, the investigation of domain structure combined with diffusion–relaxation characteristics in PIN–PMN–PT systems can facilitate the design and exploration of new high-performance ferroelectric materials.

In this work, we prepared the PIN–PMN–PT ceramics with various PIN/PMN proportions using the two-step columbite precursor method and systematically investigated their phase structure, domain structure and dielectric properties. The formation mechanism of multi-type nanoscale domain structures and strong dielectric diffusion behavior combined with PNRs' growth kinetics were discussed. In addition, the effect of PIN/PMN proportion on the domain size and dielectric diffusion–relaxation characteristics was studied. It was found that a higher PIN composition leads to a stronger dielectric diffusion characteristic and a smaller domain size. Our results indicated that regulating PIN/PMN proportion can effectively manipulate the domain size and dielectric properties in PIN–PMN–PT systems.

2. Experimental Procedure

The PIN–PMN–PT ceramics with various PIN/PMN proportions near MPB composition were prepared using the conventional two-step columbite precursor method. The starting materials of In_2O_3 (99.99% purity), MgO (99.9% purity), Nb_2O_5 (99.9% purity), PbO (99.9% purity) and TiO_2 (99% purity) were purchased from Aladdin Corporation (Shanghai, China). The precursors $InNbO_4$ and $MgNb_2O_6$ were synthesized at a suitable sintered temperature of 1100°C and 1000°C, respectively, for 7 h. Subsequently, the stoichiometrically weighed $InNbO_4$, $MgNb_2O_6$, PbO and TiO_2 were ball-milled for 24 h and then pre-fired at 850°C for 4 h. After a second ball-milling for 12 h, the pre-fired powders with a moderate amount of PVA were pressed into the pallets. Then, the PVA was dumped at 550°C for 2 h, and the samples were sintered at 1250°C for 6 h in air.

The X-ray diffraction (XRD) patterns of precursors and sintered ceramics were examined using Rigaku, D/MAX-2600/PC, and the microstructures were determined by SEM (JEOL, 6700 F). For the dielectric and ferroelectric measurements, silver electrodes were printed on both the opposite surfaces of the samples. The temperature-dependent permittivity was measured by an Agilent E4980A precision LCR meter combined with a temperature control system. For piezoresponse force microscopy (PFM) measurements, the samples were polished by a precision grinder polisher (Buehler Ecomet 250). The polished samples were annealed at 350°C for 2 h to release the surface stresses produced during the polishing processes. Then, the domain morphology was observed by PFM (Asylum Research, Cypher ES). To measure the piezoelectric performances, the samples were poled under an electric field of 40 kV/cm at 130°C for 10 min. The piezoelectric coefficient d_{33} was measured by a quasi-static ZJ-2 piezoelectric d_{33} measuring instrument. The electromechanical coupling coefficient k_p is calculated using the impedance-resonance method based on the IEEE standard.

3. Results and Discussion

3.1. *Preparation, crystal structure and microstructure*

To avoid the emergence of pyrochlore phases, the precursors of $InNbO_4$ and $MgNb_2O_6$ were pre-prepared.[5–7] Figure 1 shows the XRD patterns of $InNbO_4$ at different sintering temperatures for 7 h, fixed at a heating rate of 2°C/min. One can see that the In_2O_3 and Nb_2O_5 powders do not react completely at 900°C and 1000°C. By increasing the sintering temperature to 1100°C, the pure $InNbO_4$ precursor can be obtained[22]; thus, the appropriate sintering temperature of $InNbO_4$ is 1100°C. Figure 2(a) gives XRD patterns of

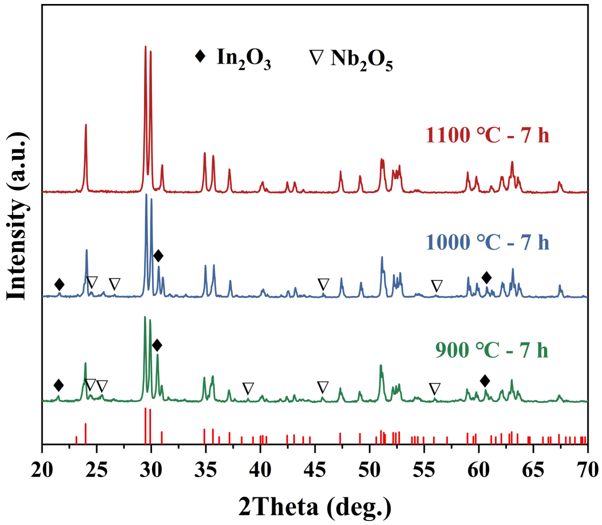

Fig. 1. XRD patterns of $InNbO_4$ precursor at different sintering temperatures.

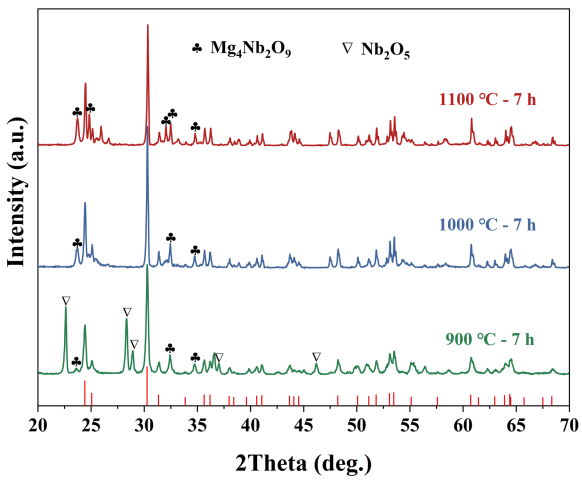

(a)

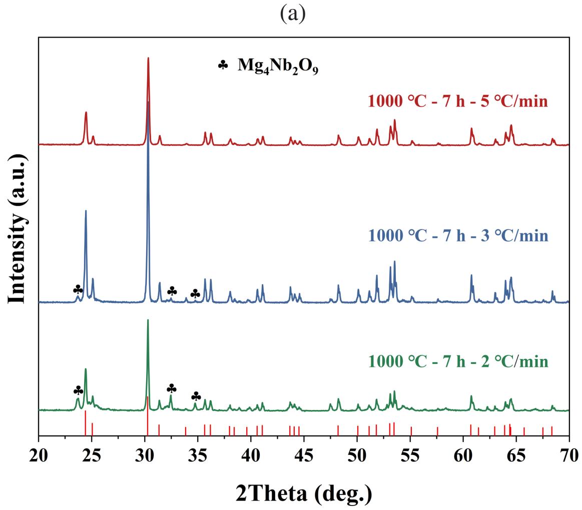

(b)

Fig. 2. (a) XRD patterns of $MgNb_2O_6$ precursor at different sintering temperatures and (b) XRD patterns of $MgNb_2O_6$ precursor at various heating rates.

$MgNb_2O_6$ at different sintering temperatures for 7 h, fixed at a heating rate of 2°C/min. It can be seen that there exist the diffraction peaks of incomplete reacting Nb_2O_5 and derivative $Mg_4Nb_2O_9$ phase at 900°C. With increasing the sintering temperature to 1000°C, the diffraction peaks of Nb_2O_5 vanish, indicating that the starting materials of MgO and Nb_2O_5 completely react. However, the $Mg_4Nb_2O_9$ phases still exist. When increasing the sintering temperature to 1100°C, the number of $Mg_4Nb_2O_9$ phases increases compared with the sample sintered at 1000°C. It is suggested that the appropriate sintering temperature of $MgNb_2O_6$ is approximately 1000°C. To acquire the pure $MgNb_2O_6$ precursor, the effect of heating rate on the $MgNb_2O_6$ sintering was investigated, as shown in Fig. 2(b). It can be observed that the $Mg_4Nb_2O_9$ phases gradually disappear with increasing the heating rate from 2°C/min to 5°C/min while fixing the sintering temperature at 1000°C. When the heating rate increases to 5°C/min, the pure $MgNb_2O_6$ can be obtained.[23] It suggests that raising the temperature to the optimum sintering temperature against time can suppress the derivative phase to acquire the pure $MgNb_2O_6$ precursors.

Figure 3(a) displays the phase diagram of ternary PIN–PMN–PT systems; a linear MPB composition region can be observed.[5,6,10] In this work, we chose the samples near the MPB composition with various PIN/PMN proportions of 6PIN–60PMN–34PT, 24PIN–42PMN–34PT and 58PIN–8PMN–34PT to implement the studies. The selected compositions are indicated by the star signs in Fig. 3(a). Selecting the samples with 34PT composition is due to their excellent dielectric and electromechanical properties.[6,24] Figure 3(b) shows XRD patterns of PIN–PMN–34PT ceramics presintered at 850°C and sintered at 1250°C.[5–10] All the samples present pure perovskite structures without the trace of the pyrochlore and other impure phases. Meanwhile, all the samples exhibit a broadened (200) peak without any obvious splitting sign, indicating that the samples possess the MPB composition with rhombohedral and tetragonal phases.[5–10]

Figure 4 gives the SEM micrographs of the fractured surface of PIN–PMN–34PT ceramics. It can be observed that all the samples exhibit good compactness with sufficient grain growth and relatively uniform grain size. Moreover, the samples exhibit the mixed mechanical fracture modes of transgranular and intergranular, resulting in partial blurry grain boundaries under the transgranular mode.[25–27] A similar phenomenon was reported in PIN–PMN–PT and other relaxor ferroelectric ceramics.[23,27,28] It is well known that piezoelectric ceramics are very brittle and generally exhibit intergranular fracture mode due to grain boundaries' weak mechanical bonding force. The intergranular fracture mode is usually accompanied by the weak mechanical properties of piezoelectric ceramics.[25] Thus, obtaining the transgranular fracture mode is an important way to improve the mechanical properties of piezoelectric ceramics. For PIN–PMN–PT ceramics, the mixed fracture mode of transgranular and intergranular under the mechanical loading can contribute

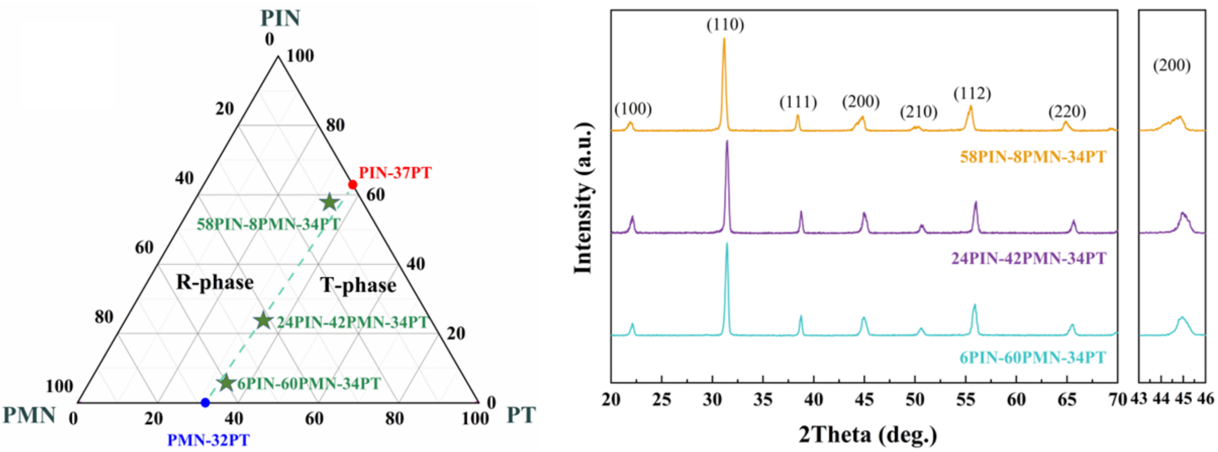

(a) (b)

Fig. 3. (a) Phase diagram of ternary PIN–PMN–PT systems and (b) XRD patterns of PIN–PMN–34PT with various PIN/PMN proportions.

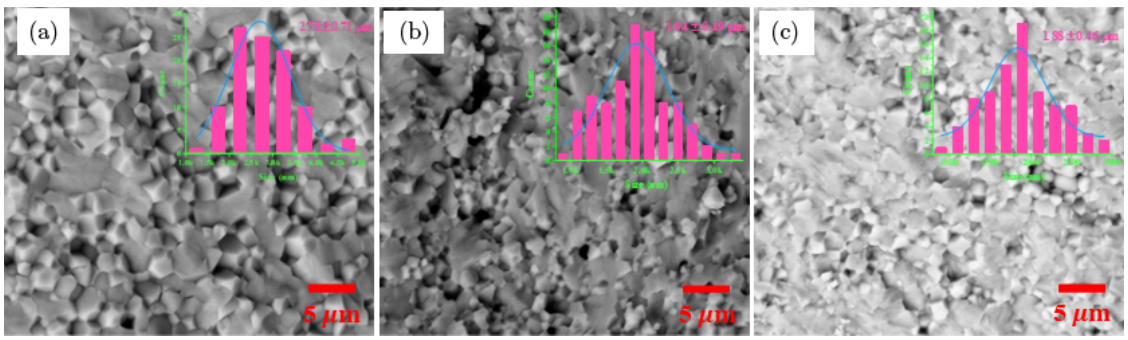

Fig. 4. SEM images of fractured surfaces of PIN–PMN–34PT ceramics (a) 6PIN–60PMN–34PT, (b) 24PIN–42PMN–34PT and (c) 58PIN–8PMN–34PT.

Table 1. Piezoelectric performances and quadratic law fitting parameters of PIN–PMN–34PT ceramics (100 kHz).

	d_{33} (pC/N)	k_p	T_A (°C)	ε_A ($10^3\varepsilon_0$)	δ (°C)	T_B (°C)	T_{CW} (°C)	ΔT_m (°C)
6PIN–60PMN–34PT	550	0.60	169	20.6	30.1	279	219	2
24PIN–42PMN–34PT	516	0.67	202	25.4	32.8	345	272	2
58PIN–8PMN–34PT	438	0.59	287	17.9	35.5	408	338	2

to excellent mechanical and electromechanical properties, particularly benefitting their high-power applications. The grain-size distribution with Gaussian fitting of PIN–PMN–34PT ceramics, using the grains with clear grain boundaries, is also given in Fig. 4. The average grain size of 6PIN, 24PIN and 58PIN samples was calculated to be 2.78 μm, 1.94 μm and 1.88 μm, respectively. It suggests that there is a slight impact on the grain size by changing the PIN/PMN proportion for PIN–PMN–PT ceramics. In addition, the piezoelectric coefficient d_{33} and electromechanical coupling coefficient k_p of poled PIN–PMN–34PT ceramics are given in Table 1. All the samples present excellent piezoelectric properties, especially for the 6PIN samples with the d_{33} = 550 pC/N and k_p = 0.60.

3.2. *Dielectric diffusion and relaxation characteristics*

Figure 5 shows the temperature-dependent dielectric constant and dielectric loss of PIN–PMN–34PT ceramics at various frequencies. It can be observed that the samples exhibit a typical DPT behavior featured by a diffuse dielectric peak and slight frequency-dependent ε_m in the vicinity of T_m. The T_m of 6PIN, 24PIN and 58PIN samples is 171°C, 211°C and 289°C, respectively. This phenomenon of a higher PIN composition inducing a higher T_m has been widely confirmed in PIN–PMN–PT systems.[5–7] Hosono *et al.* reported a linear relationship between the PIN composition and the T_m in PIN–PMN–PT ceramics.[10] In addition, there is an obvious R-phase to T-phase transition around the $T_{R\text{–}T}$ = 100°C for the 24PIN sample. However, the R–T phase transition becomes

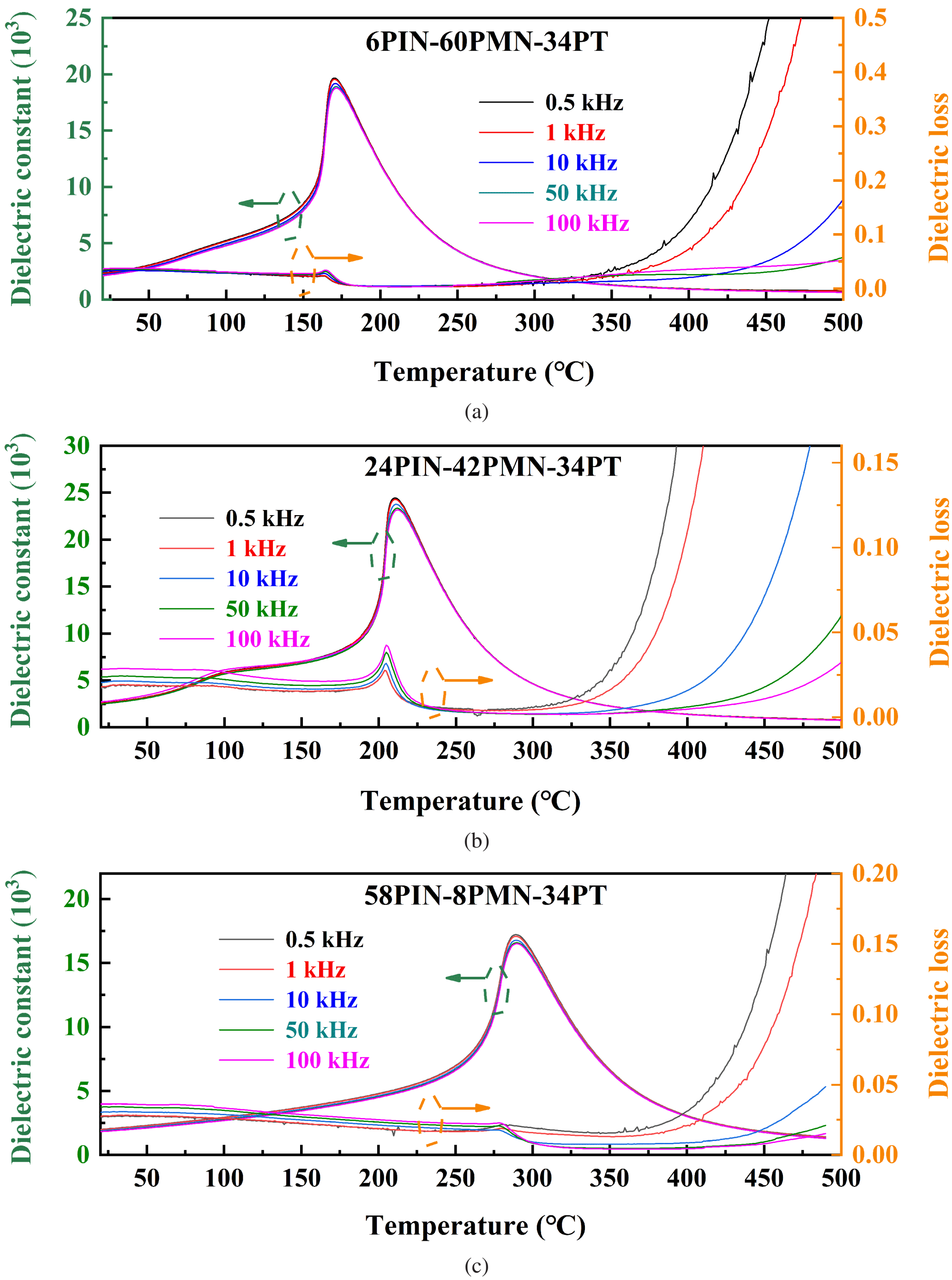

Fig. 5. Temperature-dependent dielectric constant and dielectric loss of PIN–PMN–34PT ceramics at various frequencies from 500 Hz–100 kHz, (a) 6PIN–60PMN–34PT, (b) 24PIN–42PMN–34PT and (c) 58PIN–8PMN–34PT.

weak and presents a smooth dielectric behavior in 6PIN and 58PIN samples, indicating that setting an appropriate PIN/PMN proportion can enhance the dielectric-temperature stability of PIN–PMN–PT ceramics.

It is generally known that the dielectric behavior of relaxor ferroelectrics does not obey the Curie–Weiss law above the T_m, owing to the existence of quenched PNRs embedded into the nonpolar cubic matrix at the temperature region between T_m and T_B. The T_B is the highest temperature below which PNRs exist. However, the Curie–Weiss law is still valid for relaxor ferroelectrics at $T > T_B$, as follows:[15,16]

$$\frac{1}{\varepsilon} = \frac{T - T_{\mathrm{cw}}}{C}, \tag{1}$$

where in C is the Curie–Weiss constant and T_{cw} represents the Curie–Weiss temperature; the ε and T are dielectric constant

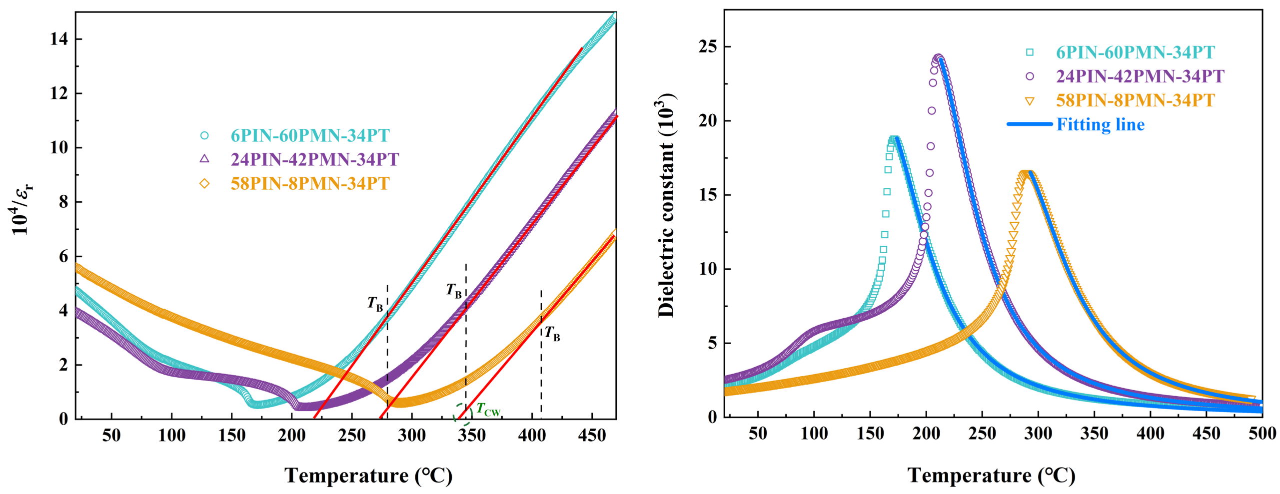

Fig. 6. (a) The temperature dependences of the inverse of the permittivity for PIN–PMN–34PT ceramics (100 kHz), (b) Lorentz-type relation fitting of the dielectric constants for PIN–PMN–34PT ceramics (100 kHz).

and temperature, respectively. Figure 6(a) shows the temperature dependences of inverse dielectric permittivity of PIN–PMN–34PT ceramics. The fitting results of the Curie–Weiss law at high temperatures are also given, and the T_B is determined. The values of T_B and T_{cw} are summarized in Table 1, and C is in the range of 10^3–10^5. One can see that the Curie–Weiss law can well describe the dielectric behavior of PIN–PMN–34PT ceramics at high temperature. The T_B increases with increasing the PIN composition due to a higher phase transition temperature T_m for the samples with higher PIN composition.

To describe the DPT behavior of PIN–PMN–34PT ceramics around T_m, a quadratic law is proposed as follows:[15,17]

$$\frac{\varepsilon_A}{\varepsilon} = 1 + \frac{(T - T_A)^2}{2\delta^2}, \tag{2}$$

where in T_A and ε_A represent the temperature and the extrapolated value of ε ($T = T_A$), respectively; δ features the degree of diffusion of the permittivity peak. A larger δ indicates a stronger diffusion of the permittivity peak. Figure 6(b) gives the relevant results of the quadratic law on the temperature-dependent dielectric constant of PIN–PMN–34PT ceramics. The fitting parameters are summarized in Table 1. One can see that the quadratic law can well fit the dielectric behaviors. The δ values of all samples are larger than 30, which is much larger than that of the binary PMN–PT system ($\delta \approx 20$) with similar PT composition.[29] In addition, the δ value increases with increasing the PIN proportion. The results suggest that a higher PIN composition can induce a stronger dielectric diffusion performance in PIN–PMN–PT systems; it is due to the own high diffusion performance of $Pb(In_{1/2}Nb_{1/2})O_3$ ($\delta > 109$).[29] However, the ΔT_m of all samples at the frequency regions from 0.5 kHz to 100 kHz is the same as 2°C, indicating the frequency-dependent $T_m(\varepsilon_m)$ behaviors of PIN–PMN–PT systems are dominated by the PT composition. According to the investigations by Liu *et al.*, the magnitude of the "T_m-frequency dependent shift" (relaxation behavior) is associated with the local interactions between the PNRs in PIN–PMN–PT systems.[30] Thus, it can be inferred that the interactions between the PNRs in PIN–PMN–PT systems mainly depend on the PT composition. Meanwhile, the PIN/PMN compositions with considerable lattice distortion determine the degree of dielectric diffusion.

The abnormal dielectric characteristics of relaxor ferroelectrics at high temperatures are closely associated with the PNRs' growth kinetics. Several studies of great significance have elucidated the nucleation and growth of PNRs by decreasing the temperature going through the T_B and T_m.[31–36] When the temperature is higher than T_B, the relaxor ferroelectrics possess a complete nonpolar cubic structure, wherein the Curie–Weiss law is valid. As decreasing the temperature to T_B, the PNRs begin to nucleate and grow, and the relaxor ferroelectrics exhibit an ER phase characterized by the unique "PNRs + nonpolar matrix" structure.[19] According to the previous studies, the number of PNRs increases with decreasing the temperature from T_B to T_m; however, the size of PNRs changes slightly.[33,34] It suggests that the temperature region from T_B to T_m is mainly associated with the nucleation process of PNRs. When the temperature decreases to T_m, the size growth of PNRs is dominant. The investigations of the PNRs' dynamics for PMN and PZN–PT systems indicated that the T_m is the phase transition temperature combined with the size growth and the amount decrease for PNRs after the phase transition.[37,38] According to the TEM results in PMN crystal, the size of PNRs increases remarkably from 10 to 20 nm combined with the decrease of PNRs' numbers in a narrow temperature range below the T_m.[38] Further decreasing the temperature from the T_m, the correlation length (r_c) among nanosized domains becomes larger, and the whole sample exhibits a local macroscopic polarized state.

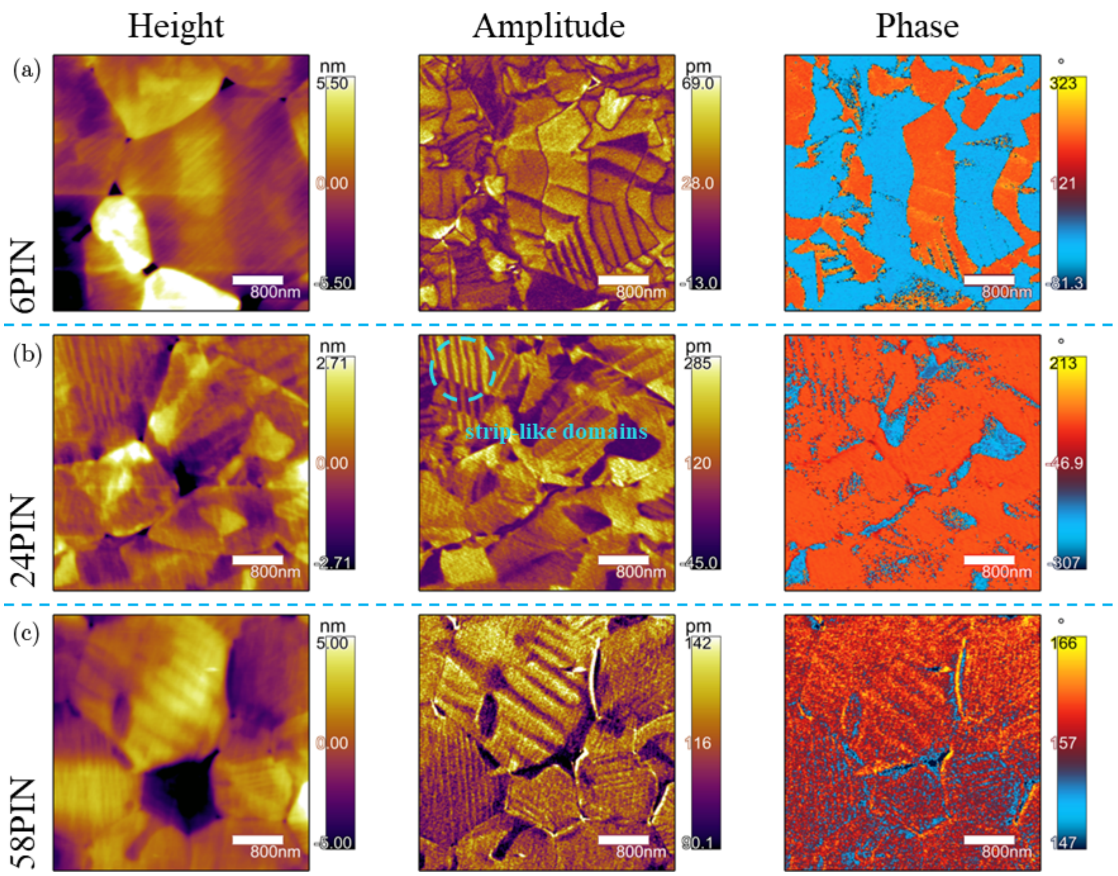

Fig. 7. PFM surface topography, amplitude and phase images of PIN–PMN–34PT ceramics at room temperature, (a) 6PIN–60PMN–34PT, (b) 24PIN–42PMN–34PT and (c) 58PIN–8PMN–34PT.

It should be noted here that the "PNRs + nonpolar matrix" is an effective model for typical PMN relaxors; however, it is not accurate for high-performance PMN–PT and PIN–PMN–PT relaxor ferroelectrics at low temperatures.[19] In these cases, the "nanosized domains + high density domain walls" model is more accurate in characterizing high-performance relaxor-based ferroelectrics due to their macroscopic polarized state (ferroelectric phase) abandoning the nonpolar matrix at low temperature.[19,39] The unique "nanosized domains + high density domain walls" structure has been widely proposed to explain the origin of ultrahigh piezoelectricity in relaxor ferroelectrics.[19] Therefore, the dielectric characteristics of PIN–PMN–PT are closely associated with the nucleation and growth of their nanosized ferroelectric domains (they can be described as the PNRs when embedded into the nonpolar matrix at high temperature).

Figures 7(a)–7(c) show the PFM images of PIN–PMN–34PT ceramics at room temperature. In the surface topography images, the surface smoothness fluctuation of the samples is lower than 5 nm. From the amplitude and phase images, it can be found that the samples exhibit the interlocking multi-type domain pattern comprising irregular island domains and regular lamellar domains at the nanoscale. Based on the underlying structure properties, the domain state of relaxor ferroelectrics with lattice distortions is strongly dependent on the local random electric fields (REFs) and the interaction between the nano-polar clusters.[30,40,41] In this case, the REFs are static (or "quenched") random fields conjugate to the order parameter.[42,43] For lead-containing complex perovskites $Pb(B_1B_2)O_3$ systems, more than one chemical element with different valence states are distributed randomly in a given lattice site; therefore, the REFs form due to a certain B-site positional and charged disorders.[44,45] For classic PMN and PIN relaxors, the REFs play a central role in preventing the formation of a completely homogeneous ferroelectric polar state leading to the appearance of nanoscale polar regions. However, introduced PT composition in PMN–PT and PIN–PMN–PT favors a long-range ferroelectric order due to the interaction between nano-polar clusters.[30,41] The competition between the REFs and the interaction of nano-polar clusters determines the present multi-type nanoscale domain states in PIN–PMN–PT ceramics.

To quantitatively investigate the effect of PIN/PMN proportions on the domain sizes, an autocorrelation function method was proposed as follows:[46]

$$<C(r)> = \sigma^2 \exp[-(r/<\xi>)^{2b}], \quad (3)$$

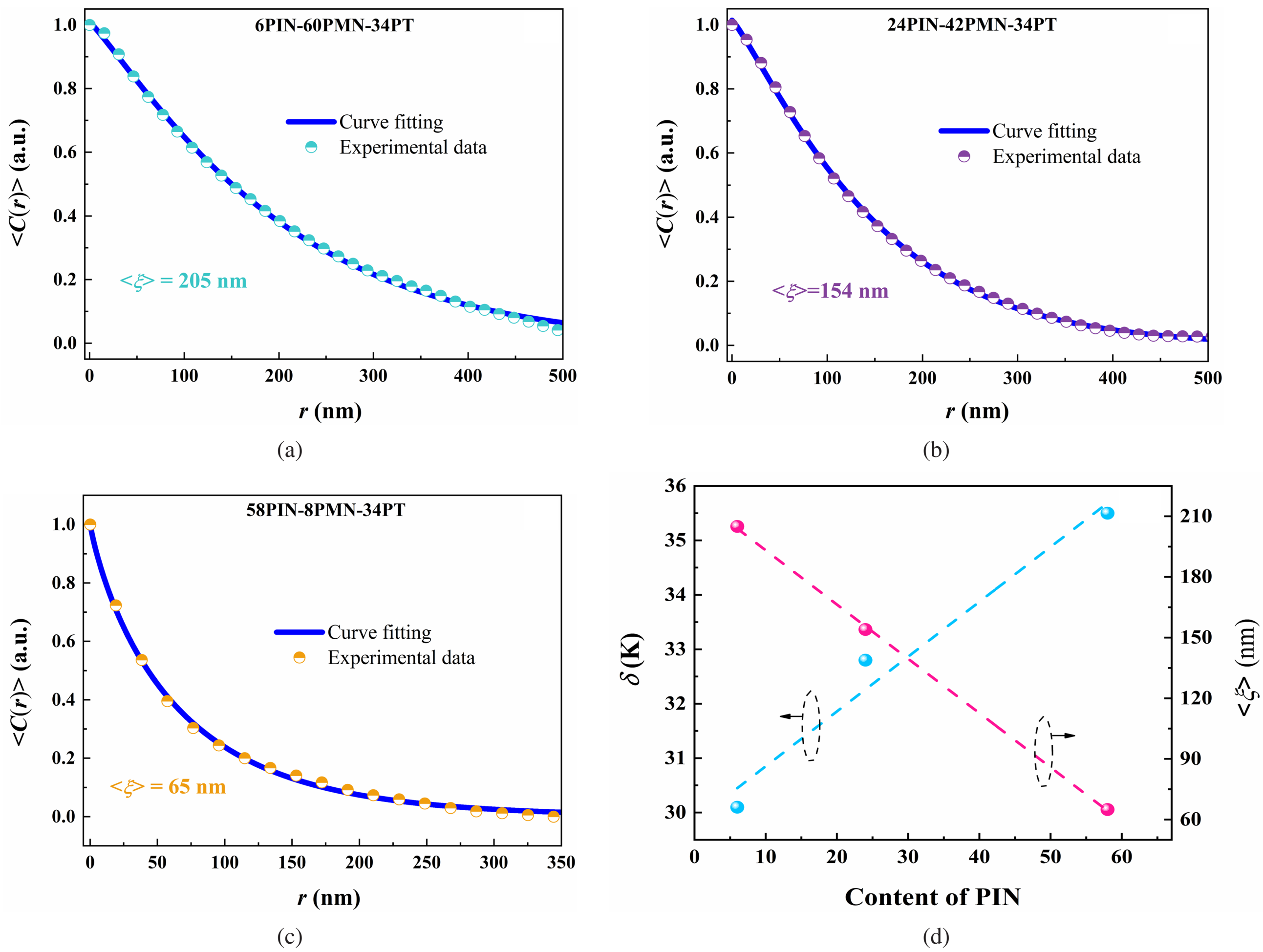

Fig. 8. (a)–(c) Autocorrelation result and average autocorrelation function $<C(r)>$ of PIN–PMN–34PT ceramics, (a) 6PIN–60PMN–34PT, (b) 24PIN–42PMN–34PT, (c) 58PIN–8PMN–34PT (d) δ and $<\xi>$ as a function of PIN proportions.

where r is the distance from the central peak, $<\xi>$ is the mean domain size representing the extent of the local polarization orientation, and b is the exponent parameter. Figures 8(a)–8(c) give the autocorrelation image and the fitting results of the average autocorrelation function. The average autocorrelation function can well fit the experimental data. The mean domain size $<\xi>$ of 6PIN, 24PIN and 58PIN samples is 205 nm, 154 nm and 65 nm, respectively. The $<\xi>$ presents a clear decrease trend with increasing the PIN proportion. Figure 8(d) shows the variations of $<\xi>$ and δ as a function of PIN proportions. It can be observed that the $<\xi>$ and δ have a linear variation tendency with increasing the PIN proportions. The results indicate that the PIN composition possesses a stronger lattice distortion than the PMN composition; therefore, increasing the PIN composition can enhance the overall structure inhomogeneity in PIN–PMN–PT systems. Meanwhile, a strong lattice distortion will enhance the REFs in the ceramic matrix, further suppressing the nucleation and growth of PNRs, leading to a stronger dielectric diffusion and a smaller domain size in the samples with higher PIN composition. Our results suggest that regulating PIN/PMN composition is an effective method for manipulating domain size and dielectric properties in PIN–PMN–PT systems.

4. Conclusions

In summary, the PIN–PMN–PT ceramics with various PIN/PMN composition proportions near the MPB were prepared by the two-step columbite precursor synthesis method. The phase structure, microstructure, dielectric diffusion–relaxation properties and domain configuration were systematically investigated. The domain structure of PIN–PMN–PT ceramics exhibits the multi-type domain patterns comprising irregular island domains and regular lamellar domains at the nanoscale. The dielectric diffusion behavior of PIN–PMN–PT systems is much stronger than that of the binary PMN–PT system with similar PT composition. In addition, the dependences of PIN/PMN proportions on the dielectric diffusion and domain size were elucidated. The results indicated that the PIN composition has a stronger lattice distortion than the PMN composition. Moreover, increasing the PIN proportion could enhance the dielectric diffusion and decrease the domain size. Our results give an in-depth understanding of structure–property relationships in PIN–PMN–PT systems and further guide the structural design of new relaxor ferroelectrics.

Acknowledgments

This research was financially supported by the National Natural Science Foundation of China (Grant No. 11974093), Open Project Program of Guangdong Provincial Key Laboratory of Electronic Functional Materials and Devices (EFMD2022006Z), and Heilongjiang Touyan Innovation Team Program (XNAUEA5640201720-09). Xudong Qi and Kai Li contributed equally to this work.

References

[1]E. W. Sun and W. W. Cao, Relaxor-based ferroelectric single crystals: Growth, domain engineering, characterization and applications, *Prog. Mater. Sci.* **65**, 124 (2014).

[2]H. Xu, B. Wang, J. Qi, M. Liu, F. Teng, L. L. Hu, Y. Zhang, C. Q. Qu and M. Feng, Modulation of spin dynamics in Ni/Pb($Mg_{1/3}Nb_{2/3}$)-O_3–$PbTiO_3$ multiferroic heterostructure, *J. Adv. Ceram.* **11**, 515 (2022).

[3]F. Li, D. B. Lin, Z. B. Chen, Z. X. Cheng, J. L. Wang, C. C. Li, Z. Xu, Q. W. Huang, X. Z. Liao, L. Q. Chen, T. R. Shrout and S. J. Zhang, Ultrahigh piezoelectricity in ferroelectric ceramics by design, *Nat. Mater.* **17**, 349 (2018).

[4]X. J. Wang, Y. Huan, Y. X. Zhu, P. Zhang, W. L. Yang, P. Li, T. Wei, L. T. Li and X. H. Wang, Defect engineering of BCZT-based piezoelectric ceramics with high piezoelectric properties. *J. Adv. Ceram.* **11**, 184 (2022).

[5]D. W. Wang, M. S. Cao and S. J. Zhang, Phase diagram and properties of $Pb(In_{1/2}Nb_{1/2})O_3$–$Pb(Mg_{1/3}Nb_{2/3})O_3$–$PbTiO_3$ polycrystalline ceramics, *J. Eur. Ceram. Soc.* **32**, 433 (2012).

[6]D. B. Lin, Z. R. Li, F. Li, Z. Xu and X. Yao, Characterization and piezoelectric thermal stability of PIN–PMN–PT ternary ceramics near the morphotropic phase boundary, *J. Alloys. Compd.* **489**, 115 (2010).

[7]D. B. Lin, H. H. Chen, Z. R. Li and Z. Xu, Phase diagram and dielectric properties of $Pb(In_{1/2}Nb_{1/2})$O3-$Pb(Mg_{1/3}Nb_{2/3})O_3$-Pb-TiO_3 ceramics, *J. Adv. Dielectr.* **5**, 1550014 (2015).

[8]J. Wu, Y. F. Chang, B. Yang, S. T. Zhang, Y. Sun, F. F. Guo and W. W. Cao, Phase transitional behavior and electrical properties of $Pb(In_{1/2}Nb_{1/2})O_3$–$Pb(Mg_{1/3}Nb_{2/3})O_3$–$PbTiO_3$ ternary ceramics, *J. Mater. Sci. Mater. Electron.* **26**, 1874 (2015).

[9]Y. K. Wang, B. J. Fang, S. Zhang, X. L. Lu and J. N. Ding, Design morphotropic phase boundary composition in the $Pb(In_{1/2}Nb_{1/2})$-O_3-$Pb(Mg_{1/3}Nb_{2/3})O_3$-$PbTiO_3$ system and its performance, *Phase Transit*, **94**, 599–615 (2021), https://doi.org/10.1080/01411594.2021.1949012.

[10]Y. Hosono, Y. Yamashita, H. Sakamoto and N. Ichinose, Dielectric and piezoelectric properties of $Pb(In_{1/2}Nb_{1/2})O_3$–$Pb(Mg_{1/3}Nb_{2/3})$-O_3–$PbTiO_3$ ternary ceramic materials near the morphotropic phase boundary, *Jpn. J. Appl. Phys.* **42**, 535 (2003).

[11]X. D. Qi, Y. Zhao, E. W. Sun, J. Du, K. Li, Y. Sun, B. Yang, R. Zhang and W. W. Cao, Large electrostrictive effect and high energy storage performance of Pr^{3+}-doped PIN-PMN-PT multifunctional ceramics in the ergodic relaxor phase, *J. Eur. Ceram. Soc.* **39**, 4060 (2019).

[12]L. E. Cross, Relaxor ferroelectrics: An overview, *Ferroelectrics* **151**, 305 (1994).

[13]S. T. Misture, S. M. Pilgrim, J. C. Hicks, C. T. Blue, E. A. Payzant and C. R. Hubbard, Measurement of the electrostrictive coefficients of modified lead magnesium niobate using neutron powder diffraction, *Appl. Phys. Lett.* **72**, 1042 (1998).

[14]F. Li, Z. Xu and S. J. Zhang, The effect of polar nanoregions on electromechanical properties of relaxor-$PbTiO_3$ crystals: Extracting from electricfield-induced polarization and strain behaviors, *Appl. Phys. Lett.* **105**, 122904 (2014).

[15]X. D. Qi, E. W. Sun, K. Li, S. Y. Li, R. Zhang, B. Yang and W. W. Cao, Dielectric relaxation properties of $[001]_{c}$-, $[011]_{c}$-, and $[111]_{c}$-oriented 0.24PIN-0.47PMN-0.29PT single crystals, *J. Am. Ceram. Soc.* **102**, 4103 (2019).

[16]D. Viehland, S. J. Jang, L. E. Cross and M. Wuttig, Deviation from Curie–Weiss behavior in relaxor ferroelectrics, *Phys. Rev. B* **46**, 8003 (1992).

[17]A. A. Bokov and Z. G. Ye, Phenomenological description of dielectric permittivity peak in relaxor ferroelectrics, *Solid. State. Commun.* **116**, 105 (2000).

[18]A. Gruverman, M. Alexe and D. Meier, Piezoresponse force microscopy and nanoferroic phenomena, *Nat. Commun.* **10**, 1661 (2019).

[19]F. Li, S. J. Zhang, D. Damjanovic, L. Q. Chen and T. R. Shrout, Local structural heterogeneity and electromechanical responses of ferroelectrics: Learning from relaxor ferroelectrics, *Adv. Funct. Mater.* **28**, 1801504 (2018).

[20]L. Y. Yang, H. B. Huang, Z. Z. Xi, L. M. Zheng, S. Q. Xu, G. Tian, Y. Z. Zhai, F. F. Guo, L. P. Kong, Y. G. Wang, W. M. Lü, L. Yuan, M. L. Zhao, H. W. Zheng and G. Liu. Simultaneously achieving giant piezoelectricity and record coercive field enhancement in relaxor-based ferroelectric crystals, *Nat. Commun.* **13**, 2444 (2022).

[21]J. X. Guo, W. W. Chen, H. S. Chen, Y. N. Zhao, F. Dong, W. W. Liu and Y. Zhang, Recent progress in optical control of ferroelectric polarization, *Adv. Opt. Mater.* **9**, 2002146 (2021).

[22]L. L. Wang, S. Zhao, L. Jin, F. Li and Z. Xu, Effects of $InNbO_4$ fabrication on perovskite PIN-PMN-PT, *J. Am. Ceram. Soc.* **97**, 3110 (2014).

[23]M. Koyuncu and S. M. Pilgrim, Effects of MgO stoichiometry on the dielectric and mechanical response of $Pb(Mg_{1/3}Nb_{2/3})O_3$, *J. Am. Ceram. Soc.* **82**, 3075 (1999).

[24]M. Pham-Thi, C. Augier, H. Dammak and P. Gaucher, Fine grains ceramics of PIN–PT, PIN–PMN–PT and PMN–PT systems: Drift of the dielectric constant under high electric field, *Ultrasonics* **44**, 627 (2006).

[25]R. F. Yue, W. Z. He, F. F. An, J. Yu and G. C. Chen, Preparation of PZT-based piezoceramics with transgranular fracture mode, *Ceram. Int.* **38**, 225 (2012).

[26]S. Jiansirisomboon, K. Songsiri, A. Watcharapasorn and T. Tunkasiri, Mechanical properties and crack growth behavior in poled ferroelectric PMN–PZT ceramics, *Curr. Appl. Phys.* **6**, 299 (2006).

[27]R. H. Kraft and J. F. Molinari, A statistical investigation of the effects of grain boundary properties on transgranular fracture, *Acta Materialia* **56**, 4739 (2008).

[28]Z. Ren and Z. G. Ye, Effects of Mn-doping on PIN-PMN-PT ceramics with MPB composition, *Ferroelectrics* **464**, 130 (2014).

[29]A. A. Bokov, Y. H. Bing, W. Chen, Z. G. Ye, S. A. Bogatina, I. P. Raevski, S. I. Raevskaya and E. V. Sahkar, Empirical scaling of the dielectric permittivity peak in relaxor ferroelectrics, *Phys. Rev. B* **68**, 052102 (2003).

[30]G. Liu, L. P. Kong, Q. Y. Hu and S. J. Zhang, Diffused morphotropic phase boundary in relaxor-$PbTiO_3$ crystals: High piezoelectricity with improved thermal stability, *Appl. Phys. Rev.* **7**, 021405 (2020).

[31]G. Y. Xu, G. Shirane, J. D. Copley and P. M. Gehring, Neutron elastic diffuse scattering study of $Pb(Mg_{1/3}Nb_{2/3})O_3$, *Phys. Rev. B* **69**, 064112 (2004).

[32]I. K. Jeong, T. W. Darling, J. K. Lee, T. Proffen, R. H. Heffner, J. S. Park, K. S. Hong, W. Dmowski and T. Egami, Direct observation of the formation of polar nanoregions in $Pb(Mg_{1/3}Nb_{2/3})O_3$ using neutron pair distribution function analysis, *Phys. Rev. Lett.* **94**, 147602 (2005).

[33]P. M. Gehring, H. Hiraka, C. Stock, S. H. Lee, W. Chen, Z. G. Ye, S. B. Vakhrushev and Z. Chowdhuri, Reassessment of the Burns temperature and its relationship to the diffuse scattering, lattice dynamics, and thermal expansion in relaxor $Pb(Mg_{1/3}Nb_{2/3})O_3$, *Phys. Rev. B* **79**, 224109 (2009).

[34]M. Roth, E. Mojaev, E. Dul, P. Gemeiner and B. Dkhil, Phase transition at a nanometer scale detected by acoustic emission within the cubic phase $Pb(Zn_{1/3}Nb_{2/3})O_3$–x$PbTiO_3$ relaxor ferroelectrics, *Phys. Rev. Lett.* **98**, 265701 (2007).

[35]R. Blinc, V. Laguta and B. Zalar, Field cooled and zero field cooled 207Pb NMR and the local structure of relaxor $PbMg_{1/3}Nb_{2/3}O_3$, *Phys. Rev. Lett.* **91**, 247601 (2003).

[36]R. Blinc, J. Dolinšek, A. Gregorovič, B. Zalar, C. Filipič, Z. Kutnjak, A. Levstik and R. Pirc, Local polarization distribution and Edwards–Anderson order parameter of relaxor ferroelectrics, *Phys. Rev. Lett.* **83**, 424 (1999).

[37]J. Macutkevic, J. Banys, A. Bussmann-Holder and A. R. Bishop, Origin of polar nanoregions in relaxor ferroelectrics: Nonlinearity, discrete breather formation, and charge transfer, *Phys. Rev. B* **83**, 184301 (2011).

[38]D. Fu, H. Taniguchi, M. Itoh, S. Koshihara, N. Yamamoto and S. Mori, Relaxor $Pb(Mg_{1/3}Nb_{2/3})O_3$: A ferroelectric with multiple inhomogeneities, *Phys. Rev. Lett.* **103**, 207601 (2009).

[39]J. Hlinka, Do we need the ether of polar nanoregions?, *J. Adv. Dielectr.* **2**, 1241006 (2012).

[40]D. Viehland and Y. Chen, Random-field model for ferroelectric domain dynamics and polarization reversal, *J. Appl. Phys.* **88**, 6696 (2000).

[41]H. R. Zeng, H. F. Yu, R. Q. Chu, G. R. Li, H. S. Luo and Q. R. Yin, Spatial inhomogeneity of ferroelectric domain structure in $Pb(Mg_{1/3}Nb_{2/3})O_3$-30%$PbTiO_3$ single crystals, *Mater. Lett.* **59**, 238 (2005).

[42]Y. Imry and S. K. Ma, Random-field instability of the ordered state of continuous symmetry, *Phys. Rev. Lett.* **35**, 1399 (1975).

[43]R. Fisch, Random-field models for relaxor ferroelectric behavior, *Phys. Rev. B* **67**, 094110 (2003).

[44]D. S. Fu, H. Taniguchi, M. Itoh, S. -ya Koshihara, N. Yamamoto and S. Mori, Relaxor $Pb(Mg_{1/3}Nb_{2/3})O_3$: A ferroelectric with multiple inhomogeneities, *Phys. Rev. Lett.* **103**, 207601 (2009).

[45]N Setter, What is a ferroelectric–a materials designer perspective, *Ferroelectrics* **500**, 164 (2016).

[46]V. V. Shvartsman and A. L. Kholkin, Evolution of nanodomains in $0.9PbMg_{1/3}Nb_{2/3}O_3$-$0.1PbTiO_3$ single crystals, *J. Appl. Phys.* **101**, 064108 (2007).